

## Experimental and numerical models in landslide behaviour

Ferran PARERA<sup>1\*</sup>

<sup>1</sup>Universitat Politècnica de Catalunya, Barcelona, SPAIN

### ABSTRACT

*The contributing factors and mechanisms involved in landslides can be addressed from different perspectives, which include real cases, testing scale models and numerical modelling. The work presented in this paper focuses on the last two mentioned ways. Instabilities observed in scaled slopes will be described and analysed. Tests were performed in a transparent tank in which boundary conditions in terms of stresses, displacements, water flow and pore water pressure were controlled. The landslide motion was recorded with a digital camera and the images were processed using the Particle Image Velocimetry (PIV) technique. The experiments performed, supplemented by laboratory tests which characterize the soil behaviour, are analysed to evaluate the landslide failure development and the post-failure behaviour.*

*The small-scaled experiments are modelled using the material Point Method (MPM). This numerical technique combines a discreet system of material points, representing the moving continuum and a fixed computational mesh. Because of this duality, the method is able to simulate automatically large displacements without mesh tangling and, therefore, it is especially useful for landslide modelling.*

*The aim of this work is to advance in the knowledge of the behaviour of landslides and their interactions with protecting structures. Combining the analysis of experimental scale models and the numerical modelling is the chosen way to understand the relevant mechanisms and controlling factors.*

*In this paper, the tank and its features to control boundary conditions are described. An experiment in which the instability of a dry sandy landslide is induced is later presented and simulated by using MPM. Numerical and experimental results, derived from PIV, are compared with the aim of validating the numerical technique.*

**Keywords:** Landslides, Material Point Method, Particle Image Velocimetry.

### 1. INTRODUCTION

This work focuses on the study of landslides from the initiation of the motion to the post-failure behaviour. It involves large displacement in saturated and unsaturated soils. Two complementary lines of research are followed: reduced

physical (1g) models and numerical simulations using and developing numerical tools that allow interpreting the phenomena observed in the laboratory.

Because of the uncertainties associated with real cases and the difficulties in taking

\* presenting author

field measurements, physical scaled models have been performed to investigate the behaviour of landslides (Montrasio et al. 2015). The main advantage of scale models is the possibility of controlling the boundary conditions of the experiment as well as the properties of the materials involved. These facts simplify the numerical modelling and offer the possibility of defining interesting benchmark exercise to validate numerical codes. The main drawback of physical models lies in the scale effects. However, if the observed response is well understood at the reduced scale and the interpretation of measurements is based on well established concepts, the conclusions of the study can be extrapolated to larger scales.

Scaled experiments performed were recorded by means of a digital camera which provides correlative images describing the motion. The images are later processed by means of a Particle Image Velocimetry (PIV) technique with the aim of knowing the displacements occurred between two consecutive images taken in a given time interval. PIV was firstly developed by Adrian (1991) to evaluate the movement in fluids. Later, PIV was implemented in the field of geotechnics as a non-invasive tool for measuring displacement in the laboratory (White et al., 2003; Take and Bolton, 2004). PIV is a useful complementary technique to traditional laboratory instruments. In particular, PIV is a powerful technique to analyse the soil behaviour and the mechanisms that occur in the whole domain of the landslide (Baba, 2002).

New methods of numerical modelling are currently being developed for the interpretation and prediction of phenomena that involve large displacements. In this work, the Material Point Method (MPM) is selected as a convenient tool to simulate the deformation processes involved in

landslides. The MPM discretizes the continuous medium in a set of lagrangian material points. Each of these points contains properties of the subdomain that represents. The material points move and transport the properties information through a fixed computational grid. The governing equations are solved in the nodes of the computation mesh. This duality makes this method particularly interesting for the study of landslides because it is able to analyse the initial static conditions, such as the initiation of the failure mechanism, and post-failure behaviour.

The work presented here is part of an ongoing research project developed in the frame of a PhD thesis carried out in the Civil Engineering and Environmental Department of Universitat Politècnica de Catalunya (Spain).

## **2. METHODOLOGY**

### **2.1. Scaled experiments**

The small-scaled models are performed in a tank specially designed to reproduce different kinds of slope failures and boundary conditions including displacement constraints, water flow, pore water pressures and relative humidity in the case of unsaturated soil states

The tank is made of transparent methacrylate and glass. Its dimensions are: 1000mm long, 200mm width and 412mm height. These dimensions allow reproducing scaled landslides in an essentially 2D plane strain configuration (Figure 1).

Water can be injected from the bottom and the lateral part of the tank. In addition, rainfall can be simulated from the upper part.

The initial slope angle can be defined by the glass guillotine which can be moved manually (Figure 1). Landslide instabilities can be induced by removing the guillotine or by wetting, imposing water flow or changes in relative humidity.

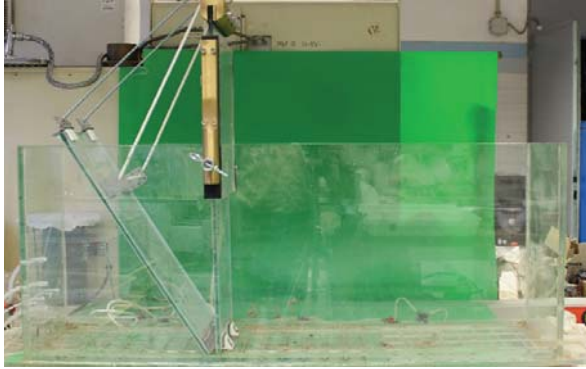


Figure 1. Tank showing the guillotine and water injection system to perform the scaled landslides.

A test programme was defined to analyse the landslide response of sand under different atmospheres equilibrated at different values of relative humidity. The effect of saturation condition on the stress-strain-strength behaviour of sands has been extensively discussed in the literature (Fraysse et al. 1999; Chen et al 2013; Fern et al. 2015). In general, increments in suction within the range investigated in this work induce increments in strength and stiffness. The work presented here will focus on the effect of non-saturation condition in fine uniform sand, and in particular, on its effect on the onset of landslide instability and the subsequent motion.

### Analysis of the results by PIV

The full process of the scaled landslide, from failure initiation to a new equilibrated state, is recorded in HD at 50 frames per second. The frames are extracted and correlated using the Particle Image Velocimetry technique.

The technique involves comparison of two digital images of the same element captured in an interval time ( $\Delta t$ ). The changes between the first image and the second one are analyzed to obtain a set of relative displacement vectors. In this work, the free-commercial software PIVLab (Thielicke et al. 2014) developed at the Groningen University (Netherlands) was selected. The images are processed and encoded in patterns to be compared

(Figure 2). The area of interest of the image  $t_1$  is divided in a mesh of interrogation sub-areas. The code analyzes geometrical and colour patterns of each sub-area of the image  $t_1$ , and searches its corresponding counterpart in the image  $t_2$ . The search-area extends a distance  $S_{max}$  beyond the area of initial interrogation. This procedure is performed for all sub-areas of interrogation image  $t_1$ .

This technique can be applied to series of images to analyze the evolution of the displacement vector field during a time interval. Notice that this methodology provides displacements vectors computed from two correlated images in points fixed in the space instead of giving the motion of a given point, which is the outcome of a numerical code based on finite element techniques. In order to compare the results obtained from PIV with numerical results an auxiliary code was written to analyze the sequence of displacement vector fields and to calculate the accumulated displacement of materials points and the associated volumetric and shear strains.

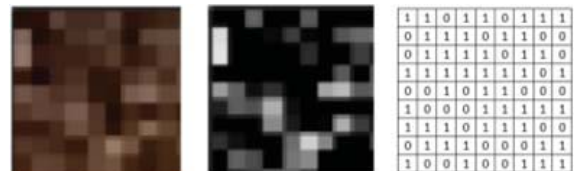


Figure 2. Ideal example of a codification in patterns in the PIV technique. Left: digital picture; center: simplified gray scaled picture; right: binary code.

## 2.2. Numerical model

### MPM methodology

The MPM method, originally called Particle-In-Cell method, was developed by Harlow et al. (1964) to be used in fluid dynamics. Later Sulsky and Schreyer extended the method to be used in soil mechanics (Sulsky et al., 1994; Sulsky et al., 1995).

In standard MPM, two levels of discretization of the media are defined:

- **Materials Points:** The continuum is discretized by means of material points that represent a portion of domain, called subdomain. The mass of the sub-domain is assumed to be concentrated in the material point and it remains constant during calculation to ensure solid mass conservation. Besides the mass, the material point contains also information of variables that change in each time step: position, velocity, strain and stress. Materials points move attached with the solid skeleton and provide the lagrangian description of the media.

- **Computational mesh:** This grid is similar to the mesh used in the Finite Element that is generated throughout the whole domain, including the space invaded by materials points during calculation even when initially are empty. The governing equations are solved in the grid nodes. The variables required for calculation and the results obtained after solving equations are transferred from nodes to materials points using mapping functions. After each time step calculation, all data is stored in the materials points and the data associated with the mesh is discarded. As a consequence, the grid remains constant throughout the calculation.

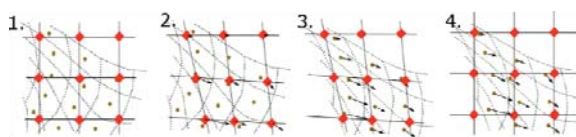


Figure 3. Scheme of the computational sequence in MPM. Material points (brown), grid nodes (red).

**Computational cycle:** The algorithm is based on the work presented by Slusky et al. (1995). A calculation cycle is divided in the following steps: (Figure 3) ( $i$  and  $j$  are associated with nodes,  $p$  is associated with materials points)

**Step 1.** From the mass information contained in the Material Points ( $m_p$ ), the nodal lumped mass matrix at time  $t^k$  ( $M$ ) is calculated using the shape function matrix ( $N_p$ ),

$$M = \sum_{p=1}^{N_p} m_p \cdot N^p \quad (1.1)$$

The internal forces ( $F^{int}$ ) are evaluated in the nodes,

$$F^{int} = \sum_{p=1}^{N_p} B^p \cdot \sigma_p V_p \quad (1.2)$$

where  $B^p$  is the nodal matrix particularized for a material point which includes the spatial derivatives of the nodal shape functions,  $V_p$  is the volume associated with each material point, and  $\sigma_p$  is the material point stress tensor.

The external forces ( $F^{ext}$ ) are evaluated on nodes following equation (1.3),

$$F^{ext} = \int_{\partial\Omega^e} N^p \cdot t d\Omega^e + \sum_{p=1}^{N_p} m_p N^p \cdot b \quad (1.3)$$

The momentum balance equation is solved and nodal accelerations ( $a_i^k$ ) are determined (1.4)

$$M^k \cdot a^k = F^{int^k} + F^{ext^k} \quad (1.4)$$

**Step 2.** The velocity at the material points ( $v_p^{k+1}$ ) is updated.

$$(2.1)$$

$$v_p^{k+1} = v_p^k + \Delta t \sum_{j=1}^{Nn} N_j^{p^k} a_j^k$$

Nodal velocities ( $v_j^{k+1}$ ) are calculated with the velocity of the material points and the nodal mass ( $m_p$ ):

(2.2)

$$v_j^{k+1} = \frac{1}{m_j^k} \sum_{p=1}^{Np} m_p N_j^{p^k} v_p^{k+1}$$

**Step 3.** Material points positions ( $x_p^{k+1}$ ) are updated,

(3.1)

$$x_p^{k+1} = x_p^k + \Delta t \sum_{j=1}^{Nn} N_j^{p^k} v_j^{k+1}$$

The strain increment of a material points ( $\Delta \epsilon_p^{k+1}$ ) can be expressed in terms of the nodal velocity ( $v_j^{k+1}$ )

(3.2)

$$\Delta \epsilon_p^{k+1} = \left( \sum_{j=1}^{Nn} B_j^{p^k} \cdot v_j^{k+1} \right) \Delta t$$

The stresses ( $\sigma$ ) are updated using a material constitutive model ( $D$ ).

(3.3)

$$\sigma = D \cdot \epsilon$$

**Step 4.** The material properties are updated in the material points.

The nodal values are discarded because all the updated information is already transferred to material points. The computational grid is initialized for the next step.

### 3. RESULTS

The comparison between the experimental and numerical results is a direct way to evaluate the performance of the numerical model. It is also an interesting way to get more information about the evolution of some parameters which are difficult to measure experimentally. Landslide failures have been induced and analysed using PIV and then modelled by MPM.

Consider a first case (A). Failure of 60° sand slope was induced by removing the guillotine. The slope dimensions are 250mm height, 200mm width and 330mm long.

The granular soil is a calcic-silicic dune sand from Castelldefels beach. The properties of the material and the slope are summarised in the Table 1.

Table 1. Sand proprieties

Sand density	1540 kg/m <sup>3</sup>
Grain density	2665 kg/m <sup>3</sup>
Porosity	0.42
Friction angle	30°
Dilatancy angle	8°
Poisson coefficient	0.3
Skeleton elastic modulus	30 MPa
Cohesion	0

The humidity of Case A was the laboratory ambient humidity (RH = 34.4%). The slope is not stable without the support provided by the guillotine. The failure starts when the guillotine is removed and the slope recover a new equilibrium after 0.9 seconds.

Figure 4 shows the evolution of the landslide. The sliding surface developing at the beginning of the experiment remains in the same place during the remaining failure stages. During the first stages of the landslide, all the points in the mobilised part have a similar velocity.

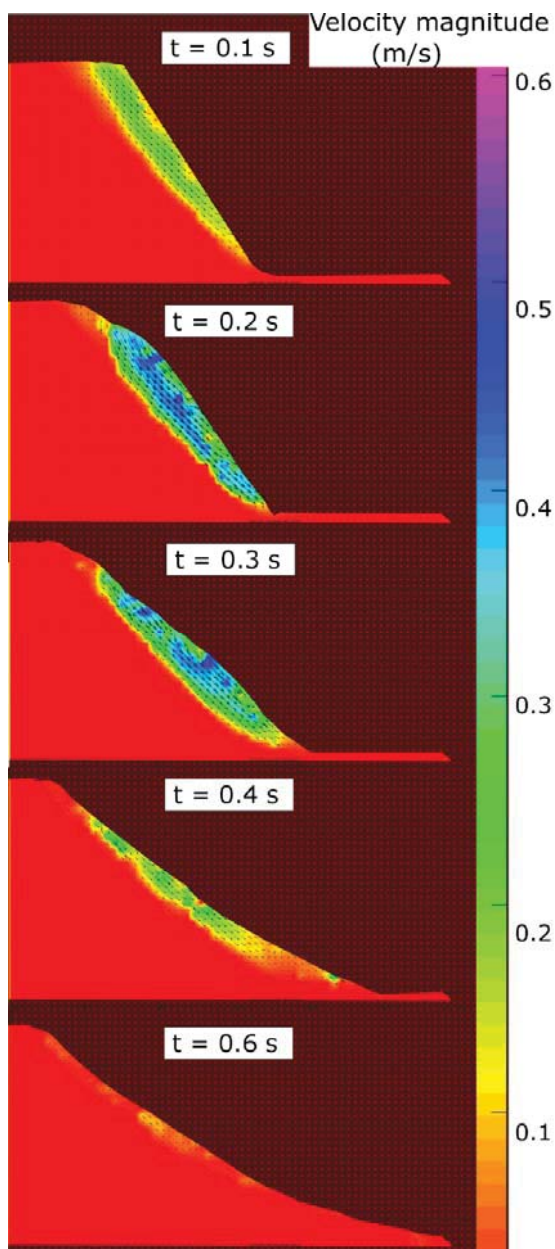


Figure 4. Velocity maps derived from the digital imaging of the failure induced in a  $60^\circ$  sand slope using a PIV technique. The color indicates the magnitude of the displacement velocity vector of each point.

However, as the landslide evolves, the velocity distribution became less homogeneous. This is a consequence of the complex granular flow established. Between times 0.2s and 0.3s, after landslide initiation, the maximum speed is reached. The average velocity in this time

interval ranges between 0.2 and 0.4 m/s. The acceleration during this period is low. This observation is interpreted as being the result of the similar values reached by the gravitational forces and the frictional and impact forces between particles which oppose the motion. In the final stage of the landslide, the effect of the accumulated flatter slope on the bottom part of the slope becomes dominant. In the image, at  $t=0.4s$  the velocity in the lower part is close 0 m/s. The stabilized slope surface becomes a curved profile having minimum inclination at the lower part and a steepest angle at the top of the slope.

### 3.1. Comparison of experimental and numerical results.

Figures 5 to 8 present a comparison between experimental and numerical results. To be able to compare both results the images have been printed with the same colour scale (each time has its own velocity scale, depending on the maximum attained speed).

The landslide behaviour predicted by the MPM model is similar to the experimental observations. The main difference lies in the velocity reached by the slope surface which is higher in the numerical model. This difference can be attributed, in part, to the difficulties of PIV techniques to calculate the velocity vectors on the model boundaries. However, the MPM simulation can also be improved. It is felt that the contact between the mobilized part of the slope and the thin stationary sand base is not properly accounted for. This is probably associated with the contact algorithm introduced in the numerical model. A final source of discrepancy may derive from the constitutive model. Granular flows imply a loss of energy by impact among particles, a phenomenon not included in the Mohr-Coulomb model adopted in the simulations performed. An additional internal dissipation would probably result in a decrease of the observed velocity.

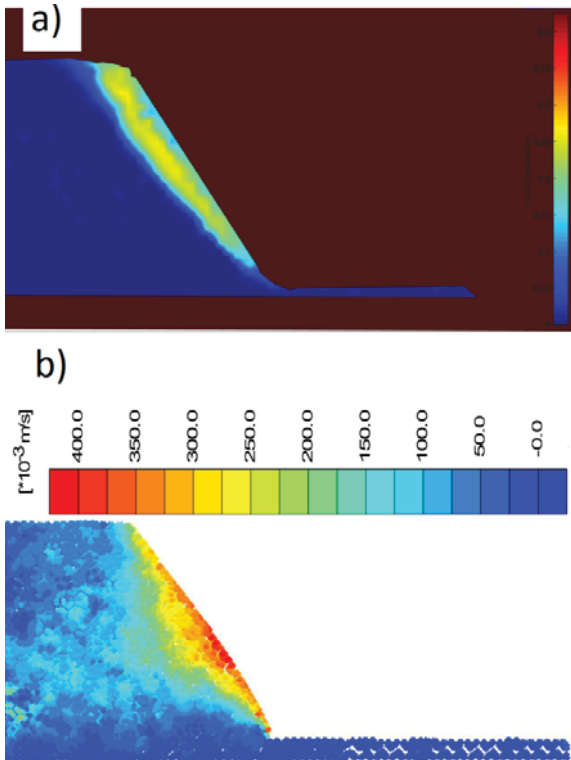


Figure 5. Comparison between experimental (a) and numerical (b) results of the velocity magnitude distribution at  $t = 0.1s$ .

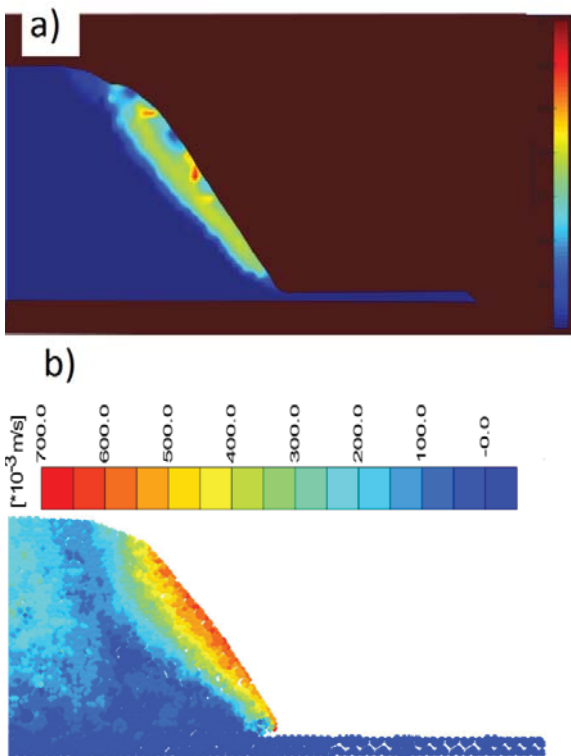


Figure 6. Comparison between experimental (a) and numerical (b) results of the velocity magnitude distribution at  $t = 0.16s$ .

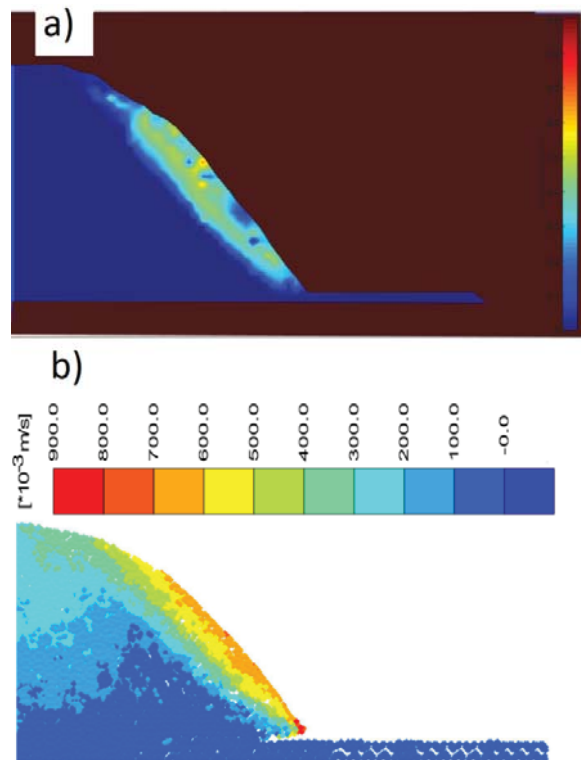


Figure 7. Comparison between experimental (a) and numerical (b) results of the velocity magnitude distribution at  $t = 0.22s$ .

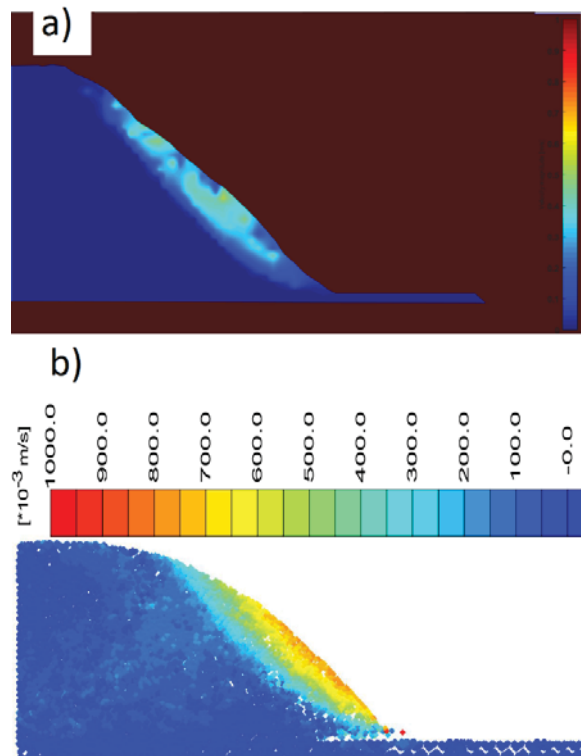


Figure 8. Comparison between experimental (a) and numerical (b) results of the velocity magnitude distribution at  $t = 0.28s$ .

#### 4. CONCLUSIONS

The comparison between the experimental and the numerical results confirms that the Material Point Method is a powerful numerical tool to analyse the behaviour of landslides.

The combination of the PIV analysis of experimental results and the MPM numerical simulation was found to be a useful procedure to test the numerical method and to suggest further developments of the code.

#### ACKNOWLEDGEMENTS

This thesis is being possible due the a FI grant from the Agency for Management of University and Research Grants (AGAUR) of Generalitat de Catalunya (Catalan government). The guidance received from the Thesis supervisors, Dr. N. Pinyol and Prof. E. Alonso is acknowledged.

#### REFERENCES

Adrian, R. J. (1991). Particle-imaging techniques for experimental fluid mechanics. *Annual review of fluid mechanics*, 23(1), 261-304.

Baba, H. O., & Peth, S. (2012). Large scale soil box test to investigate soil deformation and creep movement on slopes by Particle Image Velocimetry (PIV). *Soil and Tillage Research*, 125, 38-43.

Chen, S., Chen, L., Zhou, M., & Huang, J. (2013, December). Experimental Investigation on Factors Influencing Stable Slope Angle of Granular Accumulation. In *Applied Mechanics and Materials* (Vol. 438, pp. 1238-1243).

Fern, J., Soga, K., & Robert, D. (2015, January). Shear strength and dilatancy of partially saturated sand in direct shear tests. In *TC105 ISSMGE International Symposium on Geomechanics from Micro to Macro*, IS-

Cambridge 2014 (pp. 1391-1396). Taylor & Francis Group.

Frayssé, N., Thomé, H., & Petit, L. (1999). Humidity effects on the stability of a sandpile. *The European Physical Journal B-Condensed Matter and Complex Systems*, 11(4), 615-619.

Khalili, N., Geiser, F., & Blight, G. E. (2004). Effective stress in unsaturated soils: review with new evidence. *International Journal of Geomechanics*, 4(2), 115-126.

Montrasio, L., Schilirò, L., & Terrone, A. (2015). Physical and numerical modelling of shallow landslides. *Landslides*, 1-11.

Sulsky, D., S.-J. Zhou, and H. L. Schreyer (1995). Application of a particle-in-cell method to solid mechanics. *Computer Physics Communications*, 87(1-2):236–252.

Sulsky, D., Z. Chen, and H. Schreyer 1994. A particle method for history-dependent materials. *Computer Methods in Applied Mechanics and Engineering*, 118(1-2):179–196.

Take, W. A., Bolton, M. D., Wong, P. C. P., & Yeung, F. J. (2004). Evaluation of landslide triggering mechanisms in model fill slopes. *Landslides*, 1(3), 173-184.

Thielicke, W., & Stamhuis, E. J. (2014). PIVlab—Towards user-friendly, affordable and accurate digital particle image velocimetry in MATLAB. *Journal of Open Research Software*, 2(1), e30.

White, D. J., Take, W. A., & Bolton, M. D. (2003). Soil deformation measurement using particle image velocimetry (PIV) and photogrammetry. *Geotechnique*, 53(7), 619-632.